J Mol Model (2013) 19:2217–2224
DOI 10.1007/s00894-013-1768-1

ORIGINAL PAPER

Density functional theory studies on hydroxylamine mechanism of cyclohexanone ammoximation on titanium silicalite-1 catalyst

Chang Qing Chu · Hai Tao Zhao · Yan Ying Qi · Feng Xin

Received: 22 November 2012 / Accepted: 14 January 2013 / Published online: 31 January 2013

Abstract The hydroxylamine mechanism of cyclohexanone ammoximation on defective titanium active site of titanium silicalite-1 (TS-1) was simulated using two-layer ONIOM (M062X/6-31G**:PM6) method. A new energy favorable reaction route was found, which contained two parts: (1) the catalytic oxidation of adsorbed NH_3 to form hydroxylamine using the Ti-OOH as an active oxidant formed by reacting H_2O_2 with the defective Ti active site; (2) the subsequent noncatalytic oximation of desorbed hydroxylamine and cyclohexanone out of TS-1 pores to form cyclohexanone oxime. In the catalytic formation of hydroxylamine on the Ti active site of TS-1, the proposed mechanism of two-step single-proton transfer aided by a lattice oxygen atom bonded to Ti atom need a lower reaction energy than the mechanism proposed before. In the subsequent noncatalytic oximation of hydroxylamine and cyclohexanone, which contained two elementary reaction steps in total, the mechanisms of one-step double-proton transfer in the first elementary reaction step and the subsequent one-step three-proton transfer for the second elementary reaction step were proposed, in which the solvent water molecules played a very important role in assisting and stabilizing the proton transfer processes.

Keywords Cyclohexanone ammoximation · Density functional calculations · Hydroxylamine mechanism · ONIOM method · Titanium silicalite-1

Electronic supplementary material The online version of this article (doi:10.1007/s00894-013-1768-1) contains supplementary material, which is available to authorized users.

C. Q. Chu · Y. Y. Qi · F. Xin (✉)
Department of Chemical Engineering,
School of Chemical Engineering and Technology,
Tianjin University, Nankai District, Wei Jin Road 92,
Tianjin 300072, China
e-mail: xinf@tju.edu.cn

H. T. Zhao
Department of Chemistry, School of Science, Tianjin University,
Nankai District, Wei Jin Road 92,
Tianjin 300072, China

Introduction

The discovery of titanium silicalite-1 (TS-1) by a group at ENI [1] opened up new possibilities of developing zeolite-based green catalytic processes because TS-1 has been demonstrated to be a remarkable catalyst in the selective oxidation of a large family of organic molecules with hydrogen peroxide as an oxidant and water as the sole byproduct. The liquid-phase ammoximation of cyclohexanone over TS-1 in the presence of NH_3 and H_2O_2 to synthesize oxime, which was developed by Enichem [2] three decades ago, is one of important processes attracting the industrial interests as cyclohexanone oxime is the key intermediate in the manufacture of caprolactam which can be used to produce Nylon-6. Being the second most widely used polyamide in the world [3], Nylon-6 and its manufacturing allow cyclohexanone oxime to become a highly demanded intermediate and thus of excellent market value. Compared with the conventional technology of oxime production, the liquid-phase ammoximation of cyclohexanone over TS-1 in the presence of NH_3 and H_2O_2 to synthesize oxime shows various advantages, such that only one step is involved, without use of environmentally undesirable chemicals like oleum, halides, and oxide of nitrogen, and only a small amount of by-products are formed. Despite the excellent catalytic performances reported by several groups using TS-1 zeolite, the deactivation of TS-1 catalyst cannot be ignored [4]. Ammoximation was once considered to proceed through a TS-1-catalyzed oxidation of an intermediate of cyclohexylimine formed by the noncatalytic reaction of cyclohexanone with ammonia [5]. However, imine species formed, which is unstable and tends to decompose back to a ketone in the

presence of a large amount of H_2O which is contained inevitably in aqueous H_2O_2 and coproduced during reactions, thus, the imine species with a too-short lifetime is hard to diffuse through TS-1 pores to interact with the Ti-OOH species to give the oxime. So this mechanism was generally considered to play a minor role in the ammoximation of cyclohexanone over TS-1. The most accepted mechanism is to proceed through formation of hydroxylamine as a result of oxidation of ammonia with hydrogen peroxide catalyzed on the Ti active sites and the subsequent noncatalytic oximation of ketone with hydroxylamine to oxime in the homogeneous phase [6–8]. The experimental results showed that TS-1 exhibits no obvious shape selectivity for the ketones with a wide range of molecular sizes and performs high activity in the ammoximation of bulky ketones which hardly diffuse in the pores [6, 9]. In the absence of ketones, hydroxylamine was produced from ammonia over the TS-1 catalyst in the presence of hydrogen peroxide [10]. Although the latter proposed hydroxylamine mechanism has been demonstrated well by many experimental results [6–10], the more detailed reaction information at the molecule level of cyclohexanone ammoximation on TS-1 catalyst have not been known, which is helpful in solving the deactivation problem of TS-1 catalyst and designing a better catalyst for cyclohexanone ammoximation. Therefore, a detailed classification of the hydroxylamine mechanism of cyclohexanone ammoximation is not only scientifically valuable, but also industrially important for this reaction of commercial potential.

The characterization techniques have evidenced the coexistence of both regular [$Ti(OSi)_4$] and defective [$Ti(OSi)_3OH$] sites in TS-1 samples that synthesized following the original patent [1, 11, 12]. Wells and co-workers [13] carried out a density functional theory study of the propylene epoxidation mechanisms on both regular [$Ti(OSi)_4$] and defective [$Ti(OSi)_3OH$] sites and found the non-defective [$Ti(OSi)_4$] site had no catalytic activity in the propylene epoxidation reaction while the defective [$Ti(OSi)_3OH$] site possessed a high catalytic activity. A series of proposed active species [14–17] as shown in Fig. 1, were considered to be involved in oxidation reactions in the TS-1/H_2O_2 system. The diffuse refractance UV-vis (UV-vis DRS) spectra did not, however, contain information regarding the titanyl species [18]. Munakata and his co-workers [17] simulated the hydroxylamine formation on a non-defective Ti active site (tetraheral coordination site for Ti) using a 5T cluster model and Ti-O-O-Si as an oxidant but the active species Ti-O-O-Si was later found to be highly unstable when imposed by the zeolite lattice [19]. Recently, Wang and co-workers [20] experimentally proved that the 6-coordinated Ti-OOH (η2) was the oxidant in the TS-1/H_2O_2 system.

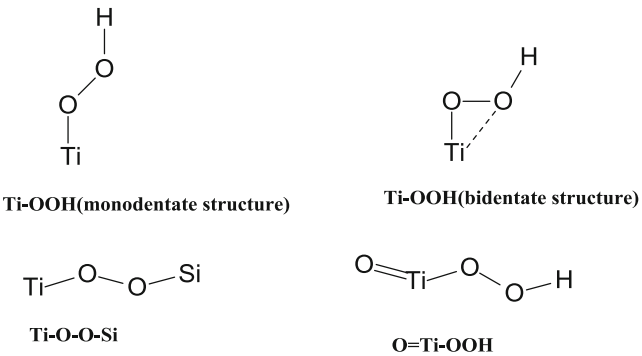

Fig. 1 Illustration of proposed oxidative active species in the TS-1/H_2O_2 reaction systems

Computational methods and cluster models

The extended 41T (a T site is a lattice Si or Ti atom tetrahedrally coordinated by four neighboring lattice O atoms) cluster model separated from the ZSM-5 zeolite lattice [21–23] was used to represent the Ti active site and the zeolite framework in this research. The dangling bonds resulted from the separation were saturated by substituting H atoms at O atom lattice positions, and adjusting Si-H bond lengths to optimized Si-H lengths at the PM6 [24] level shown in Fig. 2. This model contained a nearly circular straight channel with dimensions of 5.4–5.6 Å and a slightly elliptical zigzag channel with dimensions of 5.1–5.5 Å. Both channels intersected each other at the middle of the model. On the basis of the full *ab initio* study for determining the preferred defective [$Ti(OSi)_3OH$] sites [25], a T-9 crystallographic site (there are a total of 12 distinct crystallographically sites in the ZSM-5 zeolite lattice) was selected for Ti substitution and its nearest-neighbor Si atom at T-6 site was removed with the dangling bonds resulted from the elimination of the Si atom at T-6 site terminated with hydrogen atoms to model the defective active site. A two-layer 12T/41T ONIOM(M062X/6-31G** : PM6) method was adopted to model the properties of TS-1 and reactions occurred on it. Electronic DFT with exchange and correlation functional of M062X [26] was employed to treat the 12T region containing the Ti active site while the rest was treated by the semiempirical method PM6 to practically represent the confinement effect of the zeolite pore structure. The Los Alamos LANL2DZ [27, 28] effective core pseudopotentials (ECP) and valence double-ζ basis set were used for the titanium atom; the full double-ζ basis set plus diffuse functions, 6-31++G(d,p), was applied for the hydroxyl nest marked in Fig. 2 and all of adsorbates; 6-31G(d,p) for the rest framework atoms (Si, O, H) of the 12T region. The frequency calculations were performed on all the intermediates and transition states. All of the stable geometries with energy minimum were verified that all the frequencies were positive, and all of the transition states were verified that each had only one imaginary frequency corresponding to the vibration along the reaction pathway, furthermore, intrinsic

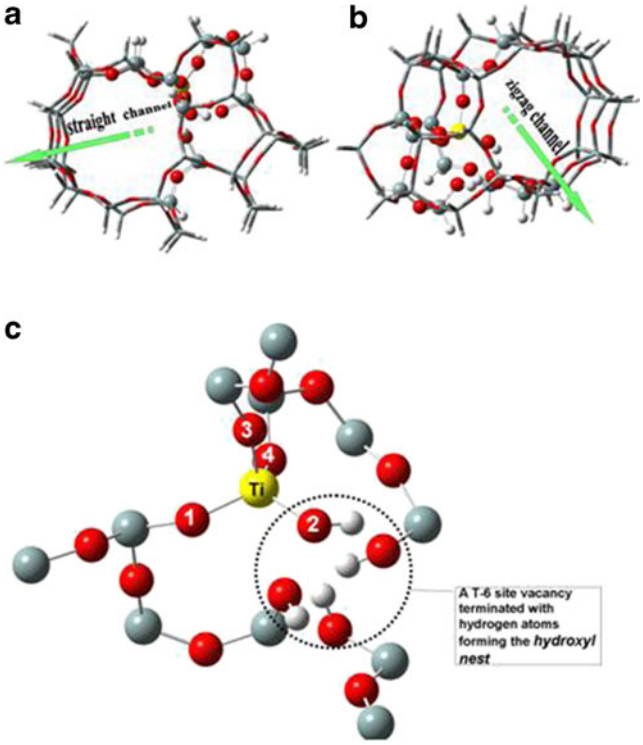

Fig. 2 The structure model used for the optimization calculation using the two-layer 12T/41T ONIOM(M062X/6-31G**:PM6) method. The high-level region is displayed with balls and sticks and the low level region is denoted by tubes **a** shows the straight channel; **b** shows the zigzag channel; **c** shows the 12T high-level region (displayed with *balls and sticks*) without the extended zeolite framework(represented by *tubes*) at the PM6 level. The atoms within the dashed circle called hydroxyl nest were calculated at the m062x/6-31++g(d,p) level

reaction coordinate (IRC) analysis was performed to further confirm that each transition state linked its corresponding reactant and product. The reaction energy barriers were reported in the electronic energy at $0K$ with zero-point-energy (ZPE) correction. Whenever reaction energy barrier was less than k_BT (k_B is Boltzmann's constant, T is absolute temperature), it was reported as negligible. All the calculations were conducted using Gaussian 09 suite of programs [29]. The optimized structural parameters of the TS-1 active site model, obtained by the method mentioned above were given in Table 1. The calculated average Ti-O bond length was 1.79 Å, which agreed with the experimental values, 1.793±0.007 Å based on XRD [30] but a little shorter than the values, 1.81±0.01 Å obtained by EXAFS [31–33].

Results and discussion

Physical adsorption of H_2O_2 on the Ti-substituted active site

In order to form the hydroperoxo species (-OOH) intermediates on the Ti active site in the TS-1 pores, H_2O_2 should first

Table 1 Selected optimized structural parameters of the TS-1 active site model calculated at the 12T/41T ONIOM(M062X/6-31G**:PM6) method level <Ti-O> represented the average Ti-O bond length

	Bond distance(Å)	Experimental values(Å)[a]
Ti-O1	1.77	
Ti-O2	1.82	
Ti-O3	1.74	
Ti-O4	1.83	
<Ti-O>	1.79	1.793±0.007, 1.81±0.01

[a] 1.793±0.007 was taken from reference [30], 1.81±0.01 was taken from reference [31–33]

diffuse through the pores and adsorb on the Ti active site. With the introduction of a H_2O_2 molecule to the defective Ti active site, it interacted with the Ti active site mainly *via* one oxygen atom (labeled as α) of the H_2O_2 molecule—***Ti_H₂O₂(ads)*** shown in Fig. 3a. The interaction between Oα and the Ti site resembled a coordinative bond with a Ti-O distance of 2.46 Å. The computed adsorption energy was exothermic by 11.2 kcal mol^{-1}, which was in line with the result obtained by an ONIOM(B3LYP/6-31g(d,p):UFF) method of 11.6 kcal mol^{-1} exothermic [34], but was much lower than that obtained in the theoretical small cluster study at the BPW91 functional of 17 kcal mol^{-1} exothermic [13]. The latter high adsorption energy (17 kcal mol^{-1}) is attributed to the use of a small quantum cluster that does not take into consideration the zeolite framework constraints. In our current reasearch, the adsorption energy for H_2O_2 to adsorb onto the 12T cluster model (see Supporting information S26) without the extended zeolite framework calculated at PM6 method level in the 41T cluster model shown in Fig. 2 was 17.1 kcal mol^{-1}.

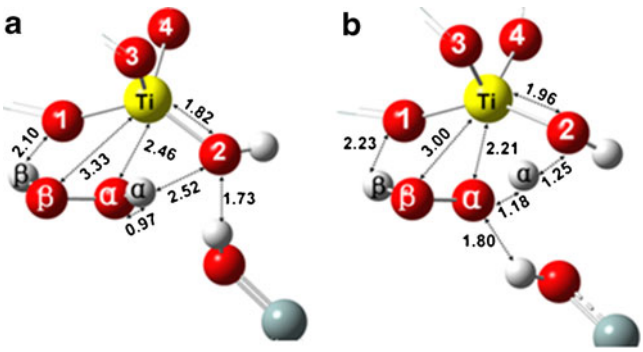

Fig. 3 **a** The physical adsorption of H_2O_2 on defective Ti active site of TS-1—TS-1_H_2O_2(ads); **b** the transition state for Ti-OOH(I) formation —Ti-OOH(TS). For clarity, some parts of the quantum region and of semi-empirical region were omitted (The color code for all figures is: *small white spheres* are hydrogen atoms; *red spheres* are oxygen atoms; *yellow sphere* is titanium atom; *greenish gray spheres* are silicon atoms; *pure gray spheres* are carbon atoms; *blue spheres* are nitrogen atoms)

Oxidative active site formation

The physisorption of H_2O_2 on the Ti active site was recently reported in an experiment conducted by Wang et al. [20], in which they proved that the Ti-OOH (η2) intermediates, not the physisorbed H_2O_2, were the active sites for propylene epoxidation. Wells et al. [19] compared the oxidative ability between the physisorbed H_2O_2 (undissociated adsorption form) and the other Ti-OOH intermediates (dissociated adsorption forms) toward propylene epoxidation by the DFT computation, and found the reaction energy barrier was much higher for the physisorbed H_2O_2 than the Ti-OOH intermediates. So, similarly, we only considered the dissociated adsorption form of H_2O_2 in the hydroxylamine formation process. In the current research, the physically adsorbed H_2O_2—***Ti_H_2O_2(ads)*** went through a transition state—***Ti-OOH(TS)*** to form the dissociated adsorption form—***Ti-OOH(I)***, which are shown in Figs. 3 and 4. The reaction energy barrier for this elementary step was 10.9 kcal mol^{-1}. The imaginary vibration mode obtained from the frequency calculation corresponded to the protonation of the titanol group. The Hα of H_2O_2 migrated directly to the titanol (-OH) group while, simultaneously, the Oα was bonding with the Ti active site. The results of this proton-transfer process were the formation of a water molecule and the titanium hydroperoxo complexes—*Ti-OOH(I)* shown in Fig. 4a. The titanium hydroperoxo complexes (Ti-OOH) formed were either in a mono (η1) or bidentate (η2) form [11, 13, 34–36]. Figure 4 shows several configurations of Ti-OOH species, the monodentate (η1) structure—***Ti-OOH(I)***, the first Ti-OOH species formed after H_2O_2 contacted with the Ti active site was the most stable one, 7.3 kcal mol^{-1} more stable than the undissociated adsorption complex ***TS-1_H_2O_2(ads)***. For the bidentate (η2) structures—***Ti-OOH(II)***, ***Ti-OOH(III)*** and ***Ti-OOH(IV)***, the ***Ti-OOH(IV)*** was the most stable one in comparison with ***Ti-OOH(II)*** and ***Ti-OOH(III)*** configuration and it was 5.6 kcal mol^{-1} more stable than the undissociated adsorption complex ***TS-1_H_2O_2(ads)***. With respect to ***TS-1_H_2O_2(ads)*** complex, the ***Ti-OOH(III)*** configuration was 3.5 kcal mol^{-1} more stable, whereas ***Ti-OOH(II)*** was found to be the least stable structure, 0.4 kcal mol^{-1} less stable.

Hydroxylamine formation

In the quantum chemical studies for the mechanism of epoxidation of ethylene [16, 37, 38], the ethylene attack at the proximal Oα (directly bonded to Ti) of the hydroperoxo species needed a much lower energy barrier than the attack at distal Oβ atom. So we only considered the NH_3 attack at the proximal Oα atom of the hydroperoxo species. As it was stated in the previous section, the water molecule which

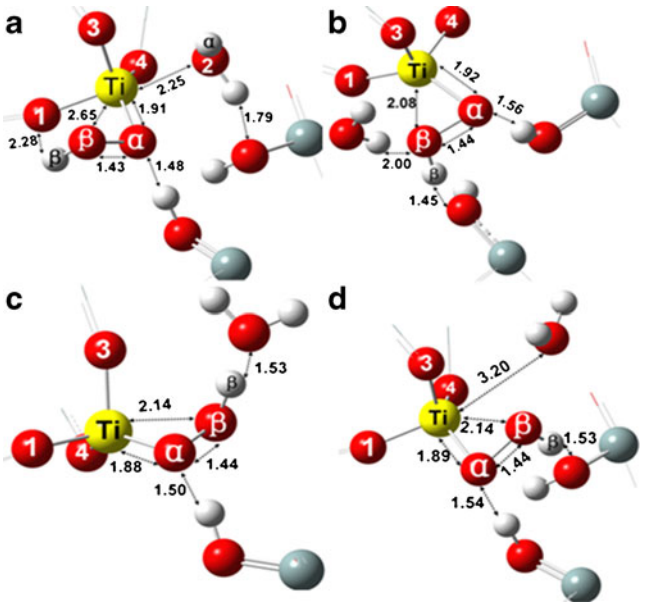

Fig. 4 **a** shows Ti-OOH(I); **b** shows Ti-OOH(II);**c** shows Ti-OOH (III); **d** shows Ti-OOH(IV). For clarity, some parts of the quantum region and of semi-empirical region were omitted

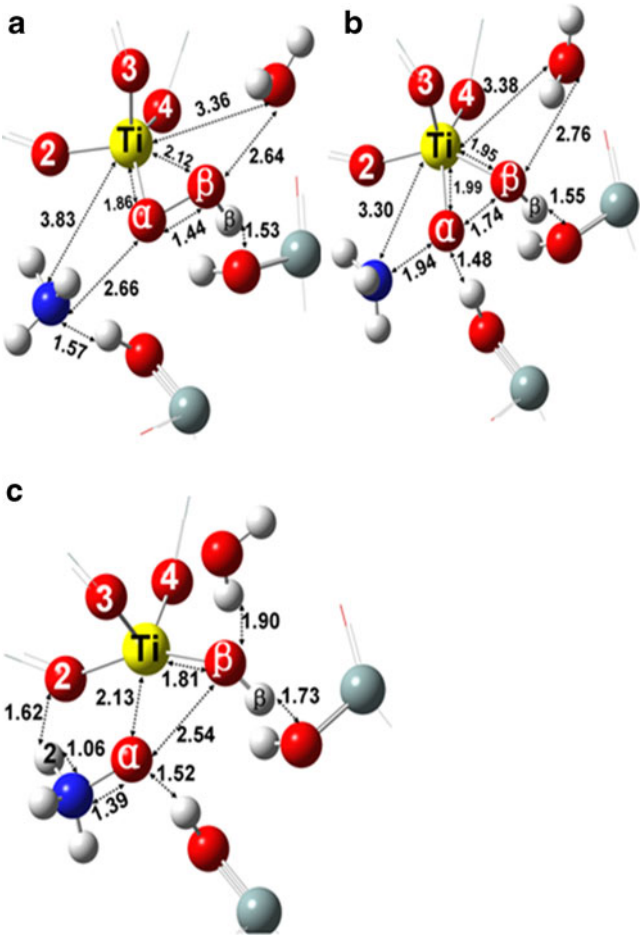

Fig. 5 **a** shows Ti-OOH(IV)_NH_3(ads); **b** shows NH_3-ONH_3(TS); **c** shows TS-1_ONH_3(ads). For clarity, some parts of the quantum region and of semi-empirical region were omitted

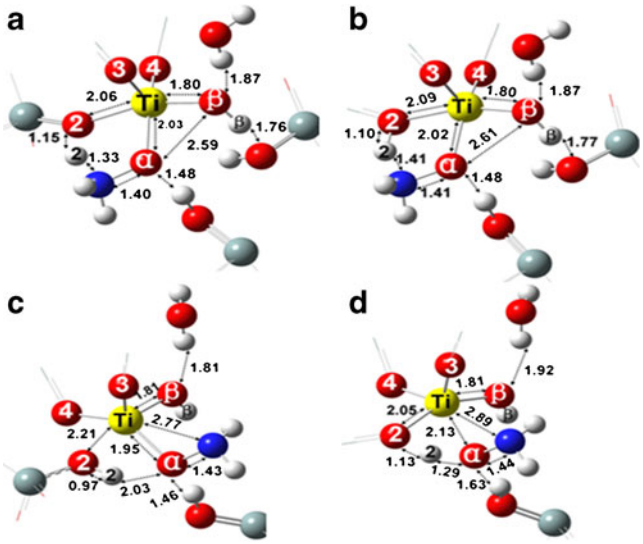

Fig. 6 **a** shows ONH3-Int(1)(TS); **b** shows Int(1); **c** shows Int(2); **d** shows Int(2)-NH_2OH(TS). For clarity, some parts of the quantum region and of semi-empirical region were omitted

formed during the formation of the ***Ti-OOH(I)***, tightly coordinated to the Ti active site next to the proximal Oα atom, so it prevented NH_3 molecule to access the active oxygen (Oα) atom of ***Ti-OOH(I)***. Recently, Wang et al. [20] experimentally proved that the Ti-OOH (η2) was the oxidant in the TS-1/H_2O_2 system. So the bidentate (η2) configurations were considered to be involved in the catalytic hydroxylamine formation process and only the bidentate (η2) ***Ti-OOH(IV)*** was chosen because it was the energetically most stable configuration among the bidentate (η2) structures but was 1.7 kcal mol^{-1} less stable than the mono (η1) *Ti-OOH (I)* (the first Ti-OOH species formed after H_2O_2 reacted with the Ti active site), and it should be noted here that the main structure differences between the mono (η1) ***Ti-OOH(I)*** and bidentate (η2) ***Ti-OOH(IV)*** were the position of the water molecule and the orientation of the –OOH group, which can be found in Fig. 4 and in the Supporting information (S4–S7). So the first formed mono (η1) ***Ti-OOH(I)*** just isomerized to the slightly less stable bidentate (η2) ***Ti-OOH(IV)*** without experiencing a transition state. After the Ti-OOH was formed by reacting a H_2O_2 molecule with the Ti active site, one NH_3 molecular came to adsorb on ***Ti-OOH(IV)*** through a hydrogen bond with one of the silanol groups of the defective site to form ***Ti-OOH(IV)_NH₃(ads)*** (Fig. 5a) and the adsorption energy was 10.9 kcal mol^{-1} exothermic. Then the next step was the oxidation of NH_3 to form an intermediate O-NH_3. From the analysis of the normal-mode coordinates of the only imaginary frequency in the transition state of NH_3 oxidation—***NH₃-ONH₃(TS)*** (Fig. 5b), the main event was the break of the Oα-Oβ of ***Ti-OOH(IV)*** and the Oα-N bond formatting. The reaction energy barrier corresponding to the transition state of NH_3 oxidizing was 23.9 kcal mol^{-1}. The resulted adsorbed intermediate ONH_3—***TS-1_ONH₃(ads)*** is shown in Fig. 5c, from which we could find that the Oα now bonding to N atom formed a coordinative bond with the Ti active site, the distance was 2.13 Å and a strong hydrogen bond 1.52 Å in length with a silanol group. Another hydrogen bond formed between the H2 and O2 with 1.62 Å in length. With the aid of the framework oxygen atom bonded to Ti active site, the intermediate ONH_3 went through a two-step single-proton transfer process to form the hydroxylamine. The first transition state structure—***ONH₃-Int(1)(TS)*** shown in Fig. 6a, led the adsorbed O-NH_3 to transform into an intermediate—***Int(1)*** shown in Fig. 6b. The first proton transfer step was a proton from the N atom to the framework O atom bonded to Ti active site. From Figs. 5 and 6, we could clearly see that in the transition process, the bond N-H2 had broken with distance from 1.06 to 1.41 Å meanwhile the bond O2-H2 was formed with distance from 1.62 to 1.10 Å. The reaction energy barrier for the first step was negligible. The

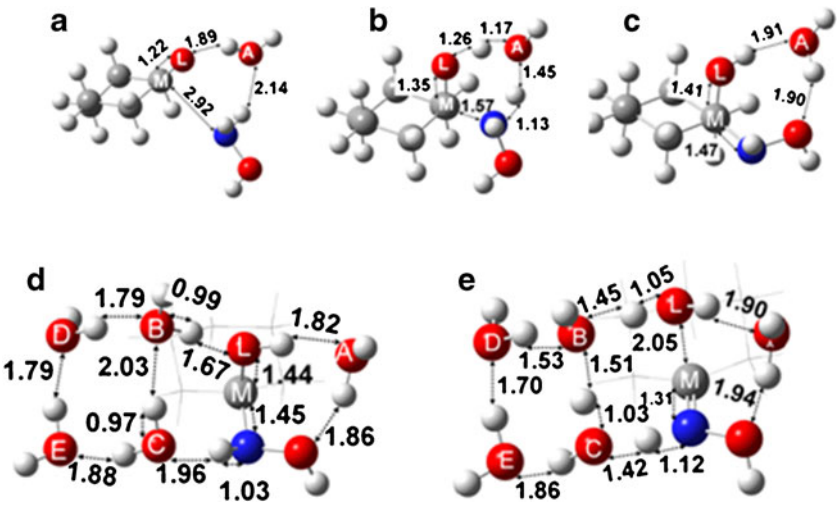

Fig. 7 **a** shows $C_6H_{10}O\_NH_2OH\_H_2O$; **b** shows $C_6H_{10}O\_NH_2OH\_H_2O$ (TS); **c** shows intermediate—Int_oximation_H_2O; **d** shows intermediate—Int_oximation_$5H_2O$ surrounded by five water molecules (labeled as *A*, *B*, *C*, *D*, *E*) **e** shows oxime_$5H_2O$(TS). For clarity, some of the atoms of the six-member ring in (**d**) and (**e**) were denoted by *lines*

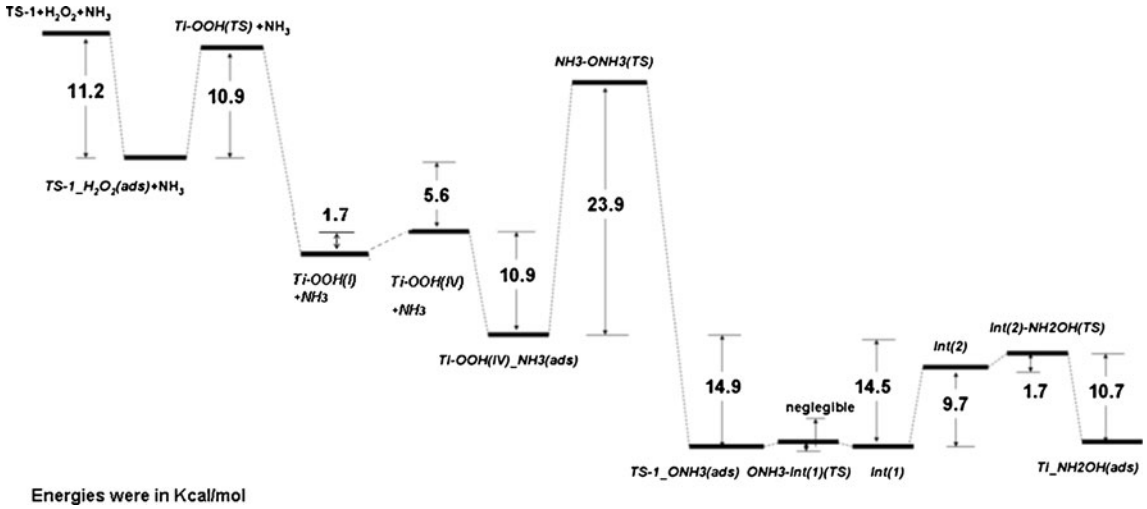

Fig. 8 Energy profile for the reaction pathway for hydroxylamine formation on defective TS-1 cluster model. The energy of the initial separate reactants (TS-1 + H_2O_2 + NH_3) was taken as the reference base (the Gibbs free energies profile was also shown in Fig. S27 in Supporting information)

intermediate ***Int(1)*** then absorbed energy of 9.7 kcal mol^{-1} experiencing a clockwise rotation to transform to another conformation—***Int(2)*** shown in Fig. 6c. The second proton transfer step was the proton transfer from O2 to Oα to finally form the hydroxylamine and the transition state ***Int (2)-NH_2OH(TS)*** is shown in Fig. 6d. The reaction energy barrier for the last step was 1.7 kcal mol^{-1}. The structure of hydroxylamine formed on the Ti active site—***Ti_NH_2OH (ads)*** was shown in the Supporting Informaton S15.

Oximation of hydroxylamine and cyclohexanone

The mechanism of ammoximation on TS-1, which consists of the catalytic formation of hydroxylamine as a result of oxidation of ammonia with hydrogen peroxide on the Ti sites and the noncatalytic oximation of ketone with hydroxylamine in the homogeneous phase to oxime, has clearly been verified by the experiments [6–8]. Furthermore, the molecule size of cyclohexanone (about 4.3 ×5.0 Å) is only slightly smaller than the sizes of TS-1 pores of 5.4 –5.6 Å (straight channel) and 5.1–5.5 Å.(zigzag channel). So it is expected that NH_2OH can diffuse more easily out of the pores into the solution than cyclohexanone diffusing into the pores since NH_2OH whose molecular size (2.5 Å) is much smaller than the pores of TS-1. The titanium zeolite-catalyzed reactions have been reported to depend greatly on the nature of the solvent used. Roffia et al. had suggested that the ammoximation over TS-1 proceeded very well in the co-solvent of H_2O and t-butanol [39] while Thangaraj et al. had shown that the best solvent for the ammoximation of cyclohexanone over TS-1 was water [5]. Wu et al. also confirmed that the best solvent for the ammoximation of cyclohexanone over Ti-MOR was water [6]. The effect of solvent is one of the most complicated issues in the catalytic system of titanosilicate/H_2O_2. So what is the role played by water in the ammoximation of cyclohexanone in the above

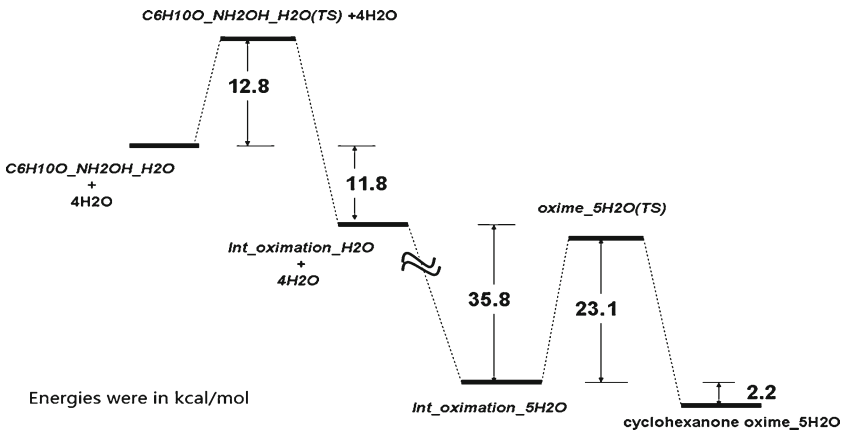

Fig. 9 Energy profile for the noncatalytic oximation of hydroxylamine and cyclohexanone. The energy of the complex $C_6H_{10}O\_NH_2OH\_H_2O$ and four isolated H_2O was taken as the reference base (the Gibbs free energies profile was also shown in Fig. S28 in Supporting information)

mentioned experiments? Based on the discussion above, we postulated NH_2OH react with cyclohexanone out of the pores of TS-1 and studied the effect of water molecules which exist in large amount as the solvent. Substitution of the hydroxylamine molecule adsorbed on the Ti active site with one H_2O_2 molecule resulted in 6.5 kcal mol^{-1} exothermic. The desorbed NH_2OH molecule then interacted with cyclohexanone through a bridge-linking H_2O molecule—***$C_6H_{10}O\_NH_2OH\_H_2O$*** shown in Fig. 7a, from which we could see that two hydrogen bonds were formed, one between the O atom of the cyclohexanone and the water molecule with 1.89 Å in length, the other one between H atom of hydroxylamine and the water molecule with 2.14 Å in length. Then the complex—***$C_6H_{10}O\_NH_2OH\_H_2O$*** went through a one-step double-proton transfer process to form the intermediate—***Int_oximation_H_2O*** shown in Fig. 7c. The transition state—***$C_6H_{10}O\_NH_2OH\_H_2O(TS)$*** is shown in Fig. 7b, the imaginary vibration mode obtained from the frequency calculation showed the synchronized dual proton-transfer mechanism where two protons, one from NH_2OH and another from water molecule, moved simultaneously toward the partial negative-charge oxygen atoms (labeled as A and L). The reaction energy barrier for the one-step double-proton transfer mechanism was 12.8 kcal mol^{-1}. The next step was the formation of cyclohexanone oxime. Besides the water molecule introduced in the first step, another four water molecules were introduced to interact with the complex ***Int_oximation_H_2O*** to form the complex ***Int_oximation_$5H_2O$*** and the five water molecules in total were labeled from A to E in alphabetical order which are shown in Fig. 7d. The transition state—***oxime_$5H_2O(TS)$*** is shown in Fig. 7e, the imaginary vibration mode obtained from the frequency calculation showed the synchronized three proton-transfer mechanism where three protons, one from N atom and two from water molecules (B and C), moved simultaneously toward the partial negative-charge oxygen atoms (labeled as B,C,L). Besides the two water molecules (B and C) whose hydrogen atoms participated in the proton transfer process, the other three water molecules (A, D and E) each formed a strong hydrogen bond with the three stranded OH groups, respectively (Fig. 7e), to greatly stabilized the proton transfer process. The reaction energy barrier was 23.1 kcal mol^{-1}. The two elementary reaction steps for oximation of hydroxylamine and cyclohexanone were also calculated without the participation of water molecules (the two transition states can be found in the Supporting information S22 and S24) and the reaction energy barriers were 31.6 and 51.7 kcal mol^{-1}, respectively, which were much higher than the situation with water molecules (12.8 kcal mol^{-1} and 23.1 kcal mol^{-1}). Energy profile for the reaction pathway of hydroxylamine formation on defective TS-1 cluster model and of the noncatalytic oximation of hydroxylamine and cyclohexanone are shown in Figs. 8 and 9, respectively.

Conclusions

Density functional theory calculations were performed to study the hydroxylamine mechanism of cyclohexanone ammoximation on defective titanium active site of titanium silicalite-1 (TS-1) catalyst. The reaction mechanism with bidentate (η2) Ti-OOH species as an oxidant which was recently experimentally proved as the oxidant in the TS-$1/H_2O_2$ system, was exploited in the postulated reaction pathways for the catalytic formation of hydroxylamine from ammonia, the two-step single-proton transfer mechanism for intermediate ONH_3 transforming to NH_2OH went through a lower reaction energy barrier than that of one-step single-proton transfer mechanism proposed by Munakata. The proposed subsequent noncatalytic oximation of hydroxylamine and cyclohexanone with water as solvent disclosed that the water molecules not only assisted the proton transferring but also stabilized this proton transferring process through hydrogen bonds.

Acknowledgments Grateful thanks for support of the National Natural Science Foundation of China (21276180) and the program for Changjiang Scholars and Innovative Research Team in University (IRT0936).

References

1. Taramasso M, Pergo G, Notari B (1983) US Patent 4,410,501
2. Roffia P, Padovan M, Leofanti G, Mantegazza MA, De Alberti G, Tamazik GR (1988) US 4,794,198
3. Parshall GW, Ittel SD (1992) Homogeneous catalysis: The applications and chemistry of catalysis by soluble transition metal complexes. Wiley, New York
4. Zhang XJ, Wang Y, Xin F (2006) Appl Catal A Gen 307:222–230
5. Thangaraj A, Sivasanker S, Ratnasamy P (1991) J Catal 131:394–400
6. Wu P, Komatsu T, Yashima T (1997) J Catal 168:400–411
7. Dal Pozzo L, Fornasari G, Monti T (2002) Catal Commun 3:369–375
8. Song F, Liu YM, Wu HH, He MY, Wu P, Tatsumi T (2006) J Catal 237:359–367
9. Zecchina A, Spoto G, Bordiga S, Geobaldo F, Petrini G, Leofanti G, Padovan M, Mantegazza M, Roffia P (1993) Stud Surf Sci Catal 75:719–729
10. Mantegazza MA, Leofanti G, Petrini G, Padovan M, Zecchina A, Bordiga S (1994) Stud Surf Sci Catal 82:541–550
11. Bordiga S, Bonino F, Damin A, Lamberti C (2007) Phys Chem Chem Phys 9:4854–4878
12. Lamberti C, Bordiga S, Zecchina A, Artioli G, Marra G, Spano G (2001) J Am Chem Soc 123:2204–2212
13. Wells DH Jr, Delgass WN, Thomson KT (2004) J Am Chem Soc 126:2956–2962
14. Sankar G, Thomas JM, Catlow CRA, Barker CM, Gleeson D, Kaltsoyannis N (2001) J Phys Chem B 105:9028–9030
15. Limtrakul J, Inntam C, Truong TN (2004) J Mol Catal A 207:139–148
16. Tantanak D, Vincent MA, Hillier IH (1998) Chem Commun 9:1031–1032
17. Munakata H, Oumi Y, Miyamoto A (2001) J Phys Chem B 105:3493–3501
18. Boccuti MR, Rao KM, Zecchina A, Leofanti G, Petrini G (1989) Stud Surf Sci Catal 48:133–144

19. Wells DH, Jr, Joshi AM, Delgass WN, Thomson KT (2006) J Phys Chem B 110:14627–14639
20. Wang LL, Xiong G, Su J, Li P, Guo HC (2012) J Phys Chem C 116:9122–9131
21. van Koningsveld H, van Bekkum H, Jansen JC (1987) Acta Crystallogr Sect B 43:127–132
22. Olson DH, Kokotailo GT, Lawton SL, Meier WM (1981) J Phys Chem 85:2238–2243
23. Kokotailo GT, Lawton SL, Olson DH, Meier WM (1978) Nature 272:437–438
24. Stewart JJP (2007) J Mol Model 13:1173–1213
25. Yuan SP, Si HZ, Fu AP, Chu TS, Tian FH, Duan Y-B, Wang JG (2011) J Phys Chem A 115:940–947
26. Zhao Y, Truhlar DG (2008) Theor Chem Acc 120:215–241
27. Hay PJ, Wadt WR (1985) J Chem Phys 82:270–284
28. Hay PJ, Wadt WR (1985) J Chem Phys 82:299–311
29. Frisch MJ, Trucks GW, Schlegel HB, Scuseria GE, Robb MA, Cheeseman JR, Scalmani G, Barone V, Mennucci B, Petersson GA, Nakatsuji H, Caricato M, Li X, Hratchian HP, Izmaylov AF, Bloino J, Zheng G, Sonnenberg JL, Hada M, Ehara M, Toyota K, Fukuda R, Hasegawa J, Ishida M, Nakajima T, Honda Y, Kitao O, Nakai H, Vreven T, Montgomery JA Jr, Peralta JE, Ogliaro F, Bearpark M, Heyd JJ, Brothers E, Kudin KN, Staroverov VN, Kobayashi R, Normand J, Raghavachari K, Rendell A, Burant JC, Iyengar SS, Tomasi J, Cossi M, Rega N, Millam NJ, Klene M, Knox JE, Cross JB, Bakken V, Adamo C, Jaramillo J, Gomperts R, Stratmann RE, Yazyev O, Austin AJ, Cammi R, Pomelli C, Ochterski JW, Martin RL, Morokuma K, Zakrzewski VG, Voth GA, Salvador P, Dannenberg JJ, Dapprich S, Daniels AD, Farkas Ö, Foresman JB, Ortiz JV, Cioslowski J, Fox DJ (2009) Gaussian 09, Revision A.1 Gaussian Inc, Wallingford, CT
30. Lamberti C, Bordiga S, Arduino D, Zecchina A, Geobaldo F, Spano G, Genoni F, Petrini G, Carati A, Villain F, Vlaic G (1998) J Phys Chem B 102:6382–6390
31. Pei S, Zajac GW, Kaduk JA, Faber J, Boyanov BI, Duck D, Fazzini D, Morrison TI, Yang DS (1993) Catal Lett 21:333–344
32. Davis RJ, Liu Z, Tabora JE, Wieland WS (1995) Catal Lett 34:101–113
33. Bordiga S, Coluccia S, Lamberti C, Marchese L, Zecchina A, Boscherini F, Buffa F, Genoni F, Leofanti G, Petrini G, Vlaic G (1994) J Phys Chem 98:4125–4132
34. Panyaburapa W, Nanok T, Limtrakul J (2007) J Phys Chem C 111:3433–3441
35. Sinclair PE, Catlow CRA (1999) J Phys Chem B 103:1084–1095
36. Barker CM, Gleeson D, Kaltsoyannis N, Catlow CRA, Sankar G, Thomas JM (2002) Phys Chem Chem Phys 4:1228–1240
37. Sever RR, Root TW (2003) J Phys Chem B 107:4090–4099
38. Yudanov IV, Gisdakis P, Di Valentin C, Rosch N (1999) Eur J Inorg Chem 1999:2135–2145
39. Roffia P, Leofanti G, Cesana A, Mantegazza M, Padovan M, Petrini G, Tonti S, Gervasutti P (1990) Stud Surf Sci Catal 55:43–52